Journal of the European Ceramic Society **6** (1990) 259–268

Crack Velocity Functions and Thresholds in Brittle Solids

Kai-Tak Wan,* Srinivasarao Lathabai*
& Brian R. Lawn‡

Ceramics Division, National Institute of Standards and Technology,
Gaithersburg, Maryland 20899, USA

(Received 27 March 1990; accepted 11 May 1990)

Abstract

A unifying treatment of environment-sensitive crack velocity functions for intrinsically brittle solids is presented. The formalism is soundly based on the concept of thermal activation barriers, but is phenomenological in that it does not attempt to identify the explicit underlying physical and chemical processes responsible for these barriers. Equations prescribing the v–G (crack velocity versus mechanical energy release rate) characteristics at specified chemical concentrations (partial pressures) and temperatures are thereby presented. These equations incorporate the familiar three velocity regions into a composite function: region I, chemically assisted fluctuations over stress-enhanced energy barriers; region III, similar but in the absence of environmental species; region II, a connecting flow-limited transport branch. In addition, the equations include provision for healing and repropagation branches in unloading–reloading cycles. Central to the argument is the assertion that zero-velocity thresholds are quiescent configurations, defined by appropriate Dupré work of adhesion terms, W. These W terms serve as reference baselines for the entire v–G function, such that changes in chemical concentration (relative humidity) or interface type (virgin versus healed) may be considered in terms of simple curve shifts along the G axis. Data for selected brittle solids, principally mica but also glass and sapphire, in moist environments are used to illustrate the formalism.

Für umgebungsabhängige Riß-Geschwindigkeits-Funktionen von spröden Materialien wird eine vereinheitlichende Betrachtungsweise vorgestellt. Die Vorgehensweise gründet sich vor allem auf das Modell der thermischen Aktivierungsschwellen, ist aber in dem Sinne phänomenologisch, als daß auf die tatsächlichen physikalischen und chemischen Prozesse, die für diese Schwellen verantwortlich sind, nicht eingegangen wird. Es werden Gleichungen aufgestellt, die den v-G Verlauf (Rißausbreitungsgeschwindigkeit gegen mechanische Energiefreisetzungsrate) bei bestimmten Konzentrationen (Partialdrücken) und Temperaturen ausdrücken. Diese Gleichungen beschreiben die bekannten drei Bereiche der Rißausbreitungsgeschwindigkeit in einer einzigen Funktion: Bereich I, chemisch unterstützte thermische Fluktuationen über spannungsabhängige Energieschwellen hinweg; Bereich III, analog, doch ohne den Einfluß des umgebenden Mediums; der die Bereiche I und III verbindende Bereich II in welchem das umgebende Medium dem Riß nur noch teilweise folgen kann. Zusätzlich schließen die Gleichungen das Ausheilen von Rissen und das erneute Fortschreiten bei Entlastungs–Wiederbelastungs-Zyklen ein. Grundlegend für alle Überlegungen ist die Annahme, daß der Punkt, an dem die Rißausbreitungsgeschwindigkeit Null wird, einen Zustand darstellt, der durch eine entsprechende Dupré-Adhäsionsarbeit, W, definiert ist. Diese W-Terme dienen als Bezugslinie für die gesamte v–G Funktion, so daß Änderungen der Konzentration (relative Feuchtigkeit) oder des Oberflächentyps (nicht angegriffen gegen ausgeheilt) als einfache Verschiebung der Kurve entlang der G-Achse betrachtet werden können. Die Vorgehensweise wird anhand der Daten ausgewählter spröder Materialien in feuchter Atmosphäre, hauptsächlich

* Permanent address: Department of Materials Science and Engineering, Lehigh University, Bethlehem, Pennsylvania 18015, USA.
‡ To whom all correspondence should be addressed.

Glimmer aber auch Glas und Saphir, exemplarisch dargestellt.

On présente ici un traitement unificateur des fonctions de vitesse de fissures sensibles à l'environnement dans le cas de solides intrinsèquement fragiles. Le formalisme est basé sur le concept des barrières d'activation thermique et est phénomènologique dans le sens où il ne tente pas d'expliquer les phénomènes physiques et chimiques sous-jacents qui sont responsables de ces barrières. On a établi des équations donnant les caractéristiques v–G (vitesse des fissures en fonction du taux de libération d'énergie mécanique) pour des concentrations chimiques (pressions partielles) et des températures déterminées. Ces équations incorporent les trois domaines de vitesse courants en une fonction composite: domaine I, fluctuations assistées chimiquement au delà des barrières d'énergie activées par les contraintes; domaine III, similaire mais avec absence d'espèces extérieures; domaine II, branche de transport de raccordement à flux limité. Ces équations incluent de plus la prévision de branches d'atténuation et de repropagation des cycles de charge–décharge. L'argument principal est que les seuils de vitesse nulle sont des configurations de repos, définies par des termes d'adhérence de Dupré, W. Ces termes W servent de base de référence pour la fonction v–G complète, de sorte que les variations de concentration chimique (humidité relative) ou de type d'interface (vierge ou traitée) puissent être considérées comme de simples décalages des courbes le long de l'axe G. On donne, pour illustrer ce formalisme, des résultats concernant des matériaux fragiles sélectionnés, principalement le mica mais également le verre et le saphir, en environnement humide.

1 Introduction

The relation between crack velocity v and mechanical energy release rate G (or stress intensity factor K) for intrinsically brittle solids in **active** environments, i.e. the v–G (or v–K) curve, provides a practical base for engineering design, especially lifetime prediction. It is therefore important to define the underlying kinetic and equilibrium states that govern this relation.

Some aspects of the crack velocity curve are relatively well documented. For instance, it is well established that, for increasing forward velocities through the virgin solid, there are three distinct 'regions', designated I, II and III, each with its characteristic dependence on G and extraneous variables such as concentration of active environmental species.

(i) *Region I*, at low velocities, depends sensitively on G and chemical activity.[1,2] This region has attracted by far the most attention in the ceramics literature. It is most often attributed to the role of intrusive active species on some crack-tip 'reaction',[1,3] but other possible mechanisms, e.g. 'lattice' diffusion in the interfacial adhesion zone just behind the crack tip[4–6] and 'internal friction' in a near-tip shielding zone,[7,8] have been proposed.

(ii) *Region II*, at intermediate velocities, also depends on environment, but is much less sensitive to G. This region is generally attributed to bulk diffusion along the crack interface behind the tip, either by free molecular flow in the gaseous state[9] or by interdiffusion in the liquid state.[10]

(iii) *Region III*, at high velocities, is again strongly dependent on G but is environment-insensitive. This region is usually associated with the kinetics of intrinsic bond rupture.[1,2]

Apart from reservations as to the true source of region I in various brittle solids, there are aspects of the general crack velocity function that are *not* well documented. Perhaps the most immediate deficiency is the lack of a unifying formalism for incorporating the various branches of the velocity function into a composite curve. There would appear to be a need for a set of working relations for specific material–environment systems, with capacity to account for the influence of concentration, temperature, etc., over the full operational range of G.

A second, and more fundamental, aspect of the crack velocity function that has received scant attention is the tendency of some v–G curves to a *threshold*, sometimes referred to as *region 0*; i.e. a G level at which the velocity cuts off to zero. The threshold remains an issue of some contention (at least in ceramics) owing to the impracticality of following cracks down to very low velocities (typically, below 1 nm s^{-1}). In principle, the proper test for existence of a threshold lies in the reversibility of crack growth: if the threshold can be regarded as a Griffith quiescent point where forward and backward fluctuations over discrete energy barriers just balance,[2,11] definable as $G = W = 2\gamma$, where W is the Dupré work of adhesion and γ is an appropriate surface energy, then at $G < W$ the crack should retract and heal; i.e. the velocity function should have a negative branch. Healing has in fact been

reported in several brittle materials, notably mica,[12,13] glass[14–16] and sapphire.[17] However, the threshold for healing and subsequent repropagation branches of the velocity curve usually occurs at a significantly lower G level than for corresponding virgin cracks, i.e. there is hysteresis in the v–G function.[5,6,13] In view of the practical implications concerning 'fatigue limits' and other such factors in lifetime predictions, it is surprising that serious attempts to incorporate threshold and hysteresis characteristics into conventional fracture mechanics formalisms are not available in the ceramics literature. This is despite the actual foreshadowing of such characteristics by Rice[18] in a classic description of equilibrium and kinetic fracture states based on irreversible thermodynamics.

In this paper the authors seek to develop a general formalism that consolidates all the branches of the v–G function, including the healing–repropagation branches. The approach will be somewhat phenomenological in the way the formalism is introduced, yet soundly based in activation theory. It will be assumed simply that the kinetics in regions I and III are attributable to discrete thermal fluctuations over energy barriers, leaving physical or chemical interpretation of these barriers to others. The crack velocities in these two regions are thereby expressible as hyperbolic sine functions of G. A feature of the formalism is that transitions in the v–G curves, e.g. from virgin to healed interfaces, can be considered in terms of shifts along the G axis, consistent with an assertion by Maugis,[8] Cook[19] and others that the adhesion energies W establish the proper reference baselines for the entire v–G function. For region II, which 'connects' regions I and III, the special case of dilute gas environments is considered, for which conditions of free molecular flow prevail. The composite velocity functions will be fitted to data for selected brittle solids, primarily mica but also glass and sapphire, in moist environments.

2 Theoretical Fracture Mechanics of Crack Velocity Function

The major features of theoretical v–G curves for intrinsically brittle solids will now be examined. The traditional separation of these curves into three kinetic branches has already been mentioned. It is important also to identify equilibrium (threshold) states, and to acknowledge the potential existence of negative (healing) and subsequent positive (repropagation) branches.

2.1 Equilibrium

As alluded to in Section 1, the Griffith condition $G = W$ defines a threshold condition for crack growth in an interactive environment.[5,6,8,11] The work of adhesion W thereby establishes a reference baseline for the entire v–G function. More specifically, W may be defined as the work to separate unit area of two solid surfaces in terms of end-point solid–solid interaction energy states, $W = U_f - U_i$; i.e. from initial (i), closed state to final (f), fully separated state.[13] For a *virgin* (v) interface, introduction of an environmental species (E) usually reduces W from its innate vacuum (0) value ${}^vW_0 = 2\gamma_S$ to ${}^vW_E = 2\gamma_{SE}$, where γ_S is the surface energy of the bulk solid and γ_{SE} the corresponding solid–fluid interface energy. Such a reduction in W may occur by virtue of adsorption, dielectric screening, capillary formation, or any other environmental interaction process that influences either (or both) U_f or U_i.[20]

In a *healed* (h) interface W can be reduced still further, to a metastable 'faulted' state ${}^hW_E < {}^vW_E$, by the interfacial trapping of an occlusion layer of environmental species during healing.[5,13]

Single-phase liquids are usually the most effective environments in reducing W_E, if only because of high chemical concentration and unrestricted mass transport. Gases can nevertheless also be effective, especially if capillary condensation occurs.[20] With the latter, W_E is expected to be a function of the partial pressure p of the active species.

2.2 Kinetics: Regions I and III for propagation in virgin solid

Consider virgin cracks. Small displacements from the Griffith equilibrium condition $G = {}^vW_E$ in environment (region I) or $G = {}^vW_0$ in vacuum (region III) cause the crack system to advance or retract at 'slow' (sub-dynamic) rates which depend on the magnitude $(G - W)$ of the perturbation (the 'motive'[8]) and on environmental variables. According to Rice,[18] such 'kinetic' crack growth is to be interpreted in terms of 'quasi-equilibrium, constrained states', describable by statically determined elastic fields but nevertheless departing from a true equilibrium condition, such that stress-enhanced fluctuations drive the crack forward (or backward) at a steady rate. The underlying key to kinetic states is the existence of atomically localised energy barriers to crack extension.

Here this notion of rate-dependent activation over energy barriers is incorporated into a phenomenological model, assuming simply that these barriers are biased by the applied stress via G. These barriers are depicted in Fig. 1 at $G > W$ (advance),

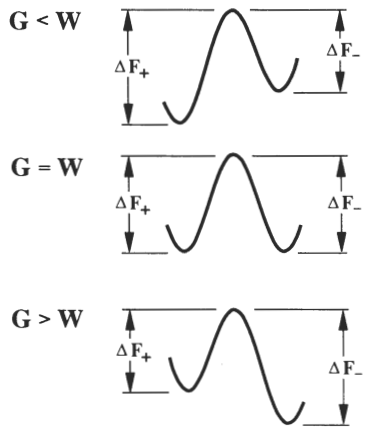

Fig. 1. Activation energy barriers to crack growth. $G > W$ (crack advance to right), $G = W$ (stationary), $G < W$ (retraction to left).

$G = W$ (stationary), and $G < W$ (retreat). The earliest model of this kind was by Wiederhorn,[1,21] specifically using reaction rate theory. The first step is to express the barrier height ΔF as a function of G. Usually, this step is arbitrarily performed as a simple Taylor expansion in stress-intensity factor.[21] Here expansion in $G - W$ is chosen instead, in order to maintain self-consistency with the Griffith balance:

$$\Delta F_{\pm} = \Delta F^{\cdot} \mp \alpha(G - W) + \cdots \qquad (G - W \ll W) \quad (1)$$

so that ΔF_+ and ΔF_- correspond to forward and backward activation, with $\Delta F^{\cdot}$ the quiescent value and $\alpha = -(\partial F/\partial G)$ an activation area. Then from classical reaction rate theory[22] the net rate of activation over the barriers is $v_0\{\exp(-\Delta F_+/kT) - \exp(-\Delta F_-/(kT)\}$, with $v_0 = kT/h$ a fundamental lattice vibration frequency, k Boltzmann's constant, h Planck's constant and T the absolute temperature. The crack velocity in regions I and III for the virgin interface is then given by the product of the activation rate and some characteristic atomic spacing a_0 between successive barriers, i.e.

$$^{v}v_{\mathrm{I}} = 2v_0 a_0 \exp(-\Delta F_{\mathrm{I}}^{\cdot}/kT) \times \sin h\{\alpha_{\mathrm{I}}(G - {}^{v}W_{\mathrm{E}})/kT\} \qquad (2a)$$

$$^{v}v_{\mathrm{III}} = 2v_0 a_0 \exp(-\Delta F_{\mathrm{III}}^{\cdot}/kT) \times \sin h\{\alpha_{\mathrm{III}}(G - {}^{v}W_0)/kT\} \qquad (2b)$$

The physics and chemistry of the activation enter the formalism via the parameters $\Delta F_{\mathrm{I}}^{\cdot}$ and $\Delta F_{\mathrm{III}}^{\cdot}$, α_{I} and α_{III}. In region III, $\Delta F_{\mathrm{III}}^{\cdot}$ and α_{III} are assumed to be determined by intrinsic bond rupture.[2] In region I, $\Delta F_{\mathrm{I}}^{\cdot}$ and α_{I} have been considered in terms of at least two rate-limiting mechanisms: crack-tip adsorption (reaction),[1,21,23] and interfacial lattice diffusion of intrusive species.[4–6] Again, the authors defer debate on such issues here.

The stress bias $G - W$ in the velocity functions in eqn (2) is emphasised as a central element in the description, regardless of specific mechanism. Note in particular that eqn (2) has natural provision for thresholds at $G = W$, and for negative velocity branches.

2.3 Kinetics: Crack propagation in healed interfaces

The kinetics of crack propagation through a healed interface will now be examined. Provided the mechanism of interaction at the crack interface remains unchanged by the occlusion,[13] eqn (1) remains a valid descriptor of the activation barriers. According to this description, the principal influence of healing is to lower the adhesion energy from $^{v}W_{\mathrm{E}}$ to $^{h}W_{\mathrm{E}}$. Hence the velocity formalism in the preceding section requires only cosmetic adjustment:

$$^{h}v_{\mathrm{I}} = 2v_0 a_0 \exp(-\Delta F_{\mathrm{I}}^{\cdot}/kT) \times \sin h\{\alpha_{\mathrm{I}}(G - {}^{h}W_{\mathrm{E}})/kT\} \qquad (3a)$$

$$^{h}v_{\mathrm{III}} = 2v_0 a_0 \exp(-\Delta F_{\mathrm{III}}^{\cdot}/kT) \times \sin h\{\alpha_{\mathrm{III}}(G - {}^{h}W_0)/kT\} \qquad (3b)$$

Consider then how a crack system undergoes a transition from virgin to healed velocity functions in a loading–unloading–reloading cycle.[5,6,13] To keep the argument simple suppose that the crack driving force is never far from equilibrium, i.e. the system is confined to region I. Initial loading drives the crack through the virgin solid along the positive branch of eqn (2a). On unloading, the crack becomes stationary at the threshold $G = {}^{v}W_{\mathrm{E}}$, and is constrained by the entrapped species to remain so until $G = {}^{h}W_{\mathrm{E}}$, at which point it retracts along the negative branch of eqn (3a) (i.e. bypassing the negative branch of eqn (2a)). On reloading above $G = {}^{h}W_{\mathrm{E}}$, the crack grows through the healed interface along the positive branch of eqn (3a).

Hence the crack system exhibits the phenomenon of *hysteresis* during the first cycle of reversed loading.

2.4 Kinetics: Region II as a connecting branch

If a crack at a given (virgin or healed) interface in a given environment is made to accelerate, the point comes where the mass flow of active species can no longer maintain pace with the tip. The adhesion zone then experiences effective 'vacuum' conditions, and the system transfers from region I to III. The connecting velocity branch defines region II.

The transport properties governing this branch depend on the nature of the environment. Liquids are not strongly transport-limited unless the viscosity is high or if the active component is present in

trace amounts.[10] Atmospheric environments, on the other hand, almost invariably show classic region II behaviour.[1,2,9] For illustrative purpose just this latter case will be dealt with.

Consider then a crack propagating at steady forward velocity v in an active atmosphere of partial pressure p. Bulk flow of the gas molecules occurs along the interface until the crack walls narrow to a separation less than that of the mean free path l of intermolecular collisions. At this point the transport rate is significantly attenuated by the dynamics of molecule–wall collisions, i.e. free molecular flow. The steady-state velocity when free molecular flow is rate limiting is given by[9]

$$v_{\mathrm{II}} = \lambda p G \tag{4}$$

where λ is a material-geometry coefficient. Evaluation of this geometry-sensitive coefficient for parabolic 'Irwin' cracks[2] yields

$$\lambda = 64 a_0^2 / 3\pi\eta E (2\pi m k T)^{1/2} \ln (l/a_0) \tag{5}$$

with η the site occupancy of adsorbate molecules per surface, m the molecular mass of the fluid species, and E Young's modulus.

The velocity in the I–II transition region will now be looked at more closely. Assuming that free molecular flow acts in *series* with the controlling process in the near-tip adhesion zone, it may loosely be written that

$$v/v_{\mathrm{I}} + v/v_{\mathrm{II}} = 1 \tag{6}$$

so that the *slowest* process is rate determining. In the same vein, the II–III transition may be considered in terms of *parallel* processes in which free molecular flow and intrinsic (vacuum) bond rupture act in concert. Then

$$v = v_{\mathrm{II}} + v_{\mathrm{III}} \tag{7}$$

so that the *fastest* process is rate determining.

Actually, this approach is oversimplistic. Strictly, the steady-state equations of free molecular flow should be solved to obtain the pressure differential $p - p*$ between crack mouth and tip,[9] and then the unknown crack-tip pressure $p*$ eliminated using an appropriate expression $W_{\mathrm{E}} = W_{\mathrm{E}}(p*)$ for the adhesion energy in eqns (2) or (3). Such flow equations[9] confirm that $p* = p$ at zero velocity configurations: at positive velocities the crack-tip pressure rapidly falls off, $p* < p$, toward zero on approaching region III; at negative velocities the pressure builds up, $p* > p$, and the crack closes (unless constrained by mechanical obstruction at the interface). In the absence of *a priori* knowledge of $W_{\mathrm{E}}(p*)$, a rigorous analysis is foregone here, but it is noted that refinements from any such analysis affect the shape of the v–G curve only in the immediate I–II and II–III transition regions.

3 Comparison with Experimental Data

The formalism in Section 2 is now illustrated with fits to available literature (plus some current) crack velocity data on selected model brittle solids. These data are presented as the individual points in Figs 2–6. The focus is on well-behaved solids with relatively simple atomic structures,[5] primarily mica,[13] the most suitable candidate material for threshold and reversibility studies because of its atomically smooth cleavage, but also silicate glass[15,16,21,24,25] and sapphire.[21] (The literature crack velocity data on glass and sapphire are usually presented as a function of stress-intensity factor K,

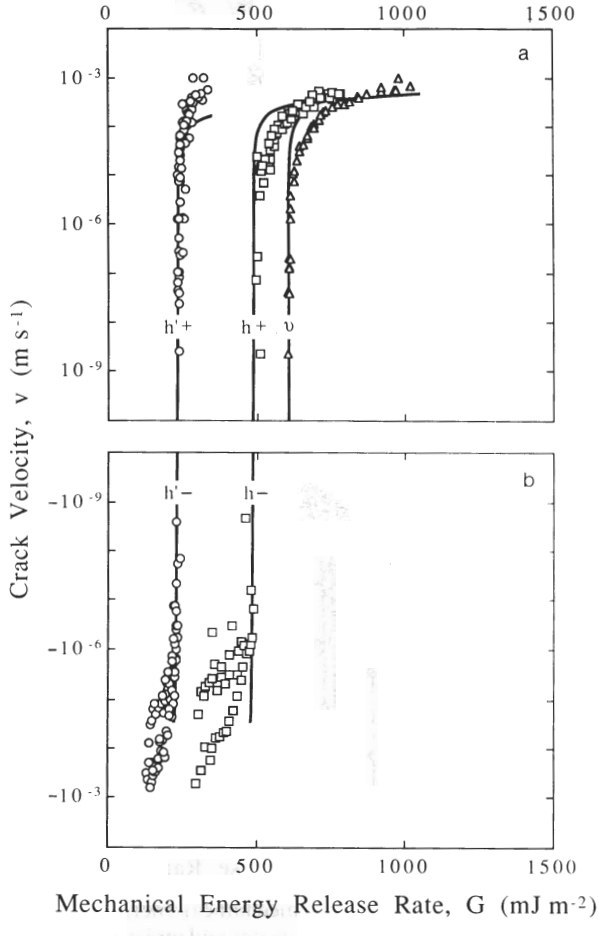

Fig. 2. Crack velocity versus mechanical energy release rate for cracks propagating in mica in air at RH 50–60%. (a) Forward (+) velocities; (b) backward (−) velocities. Data points from hysteretic loading–unloading–reloading (+/−/+) cycle; v, loading into virgin material; h, unloading–reloading along healed–matched interface; h′, same but after separating cleavage halves and misorienting about common surface normal. Data from Ref. 13, using constant-displacement double-cantilever beam geometry, at room temperature.

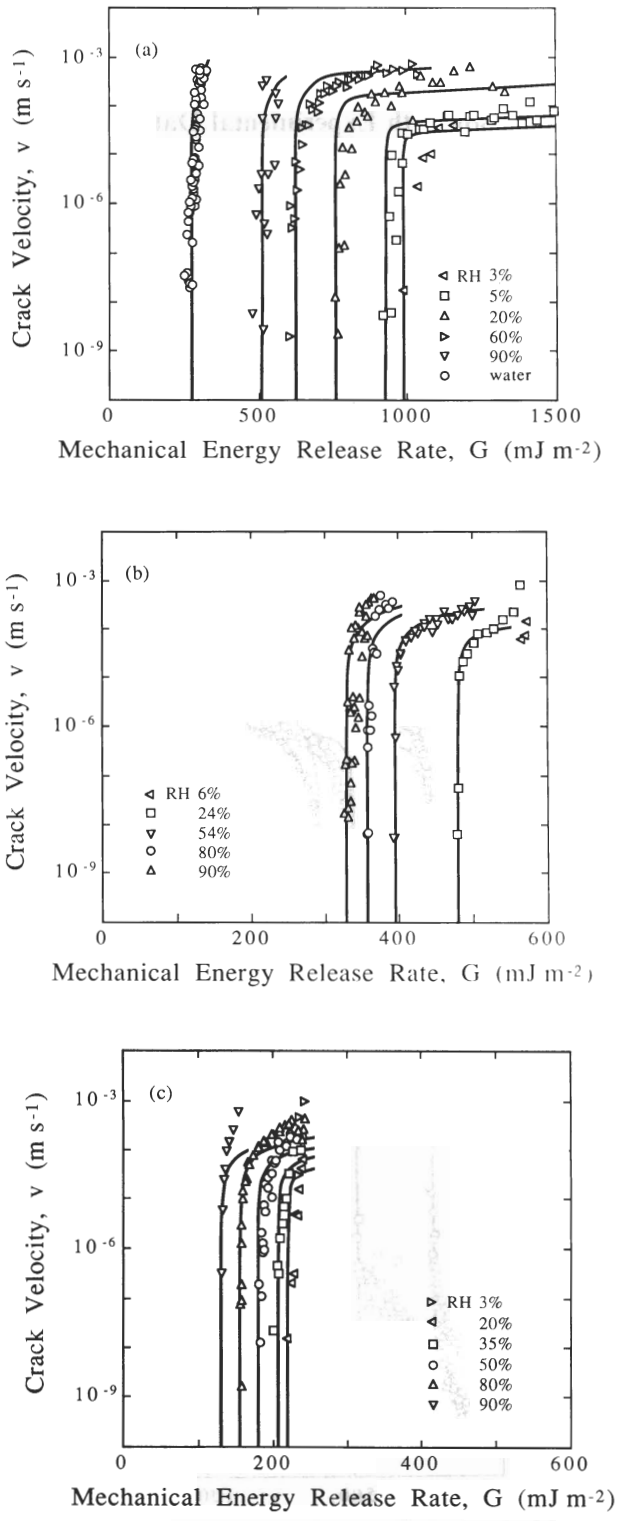

Fig. 3. Crack velocity versus mechanical energy release rate for cracks propagating in mica in water and moist air at specified RH: (a) virgin; (b) healed–matched; (c) healed–misoriented interfaces. (Note different G scales.) Data in (a) from Ref. 13, (b) and (c) current experiments using constant-displacement double-cantilever beam geometry, at room temperature.

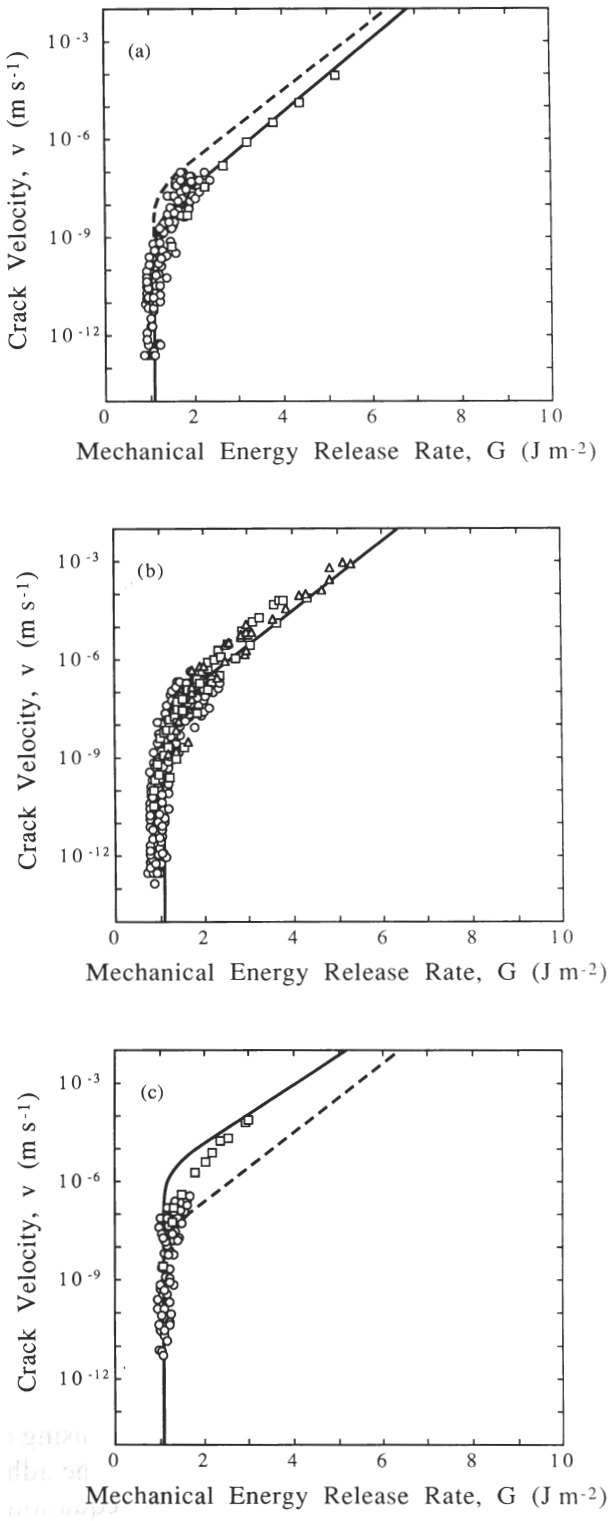

Fig. 4. Crack velocity versus mechanical energy release rate for cracks propagating in soda-lime glass in water: (a) 2–5°C; (b) 25°C; (c) 80–90°C. Constant-load double-cantilever beam data (□, Ref. 24; △, Ref. 25), plus present (stable) indentation data (○, see Appendix). Solid curves are theoretical fits (with fit at 25°C included as dashed curves in (a) and (c) to indicate data shifts).

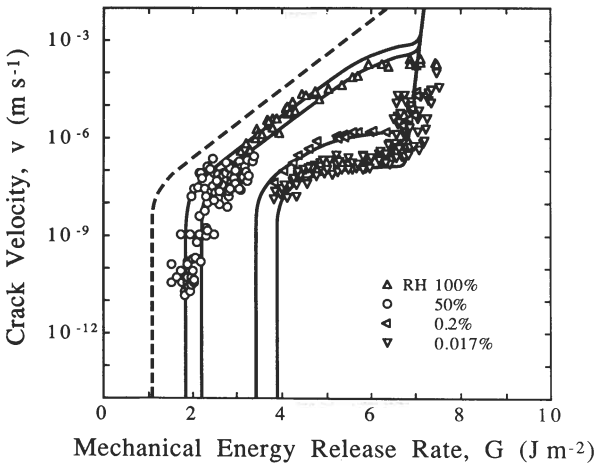

Fig. 5. Crack velocity versus mechanical energy release rate for cracks propagating in soda-lime glass in moist air at specified RH. Constant load double-cantilever beam data (△, Ref. 21), plus present indentation data (○, see Appendix), at room temperature. Solid curves are theoretical fits. (Broken curve at left is fit to room temperature water data in Fig. 4(b).)

which is converted here to G via the familiar relation $G = K^2(1-\nu^2)/E$, E = Young's modulus and ν = Poisson's ratio.) Water (liquid and vapour) as the interactive environment is also focused upon. The data for mica in Figs 2 and 3 include two types of healed interface, matched (crack carefully retracted after *partially* cleaving the specimen, to preserve lattice registry, and subsequently repropagated) and misoriented (interface recontacted after *full* separation and mutual rotation of cleavage halves before repropagation).[13] Note that none of the data sets in Figs 2–6 covers the entire spectrum of behaviour from subthreshold through region III, a reflection of limitations imposed by crack stability: stable ($dG/dc < 0$), constant-displacement geometries dispose to low velocities; conversely, unstable ($dG/dc > 0$), constant-load geometries are biased to high velocities.

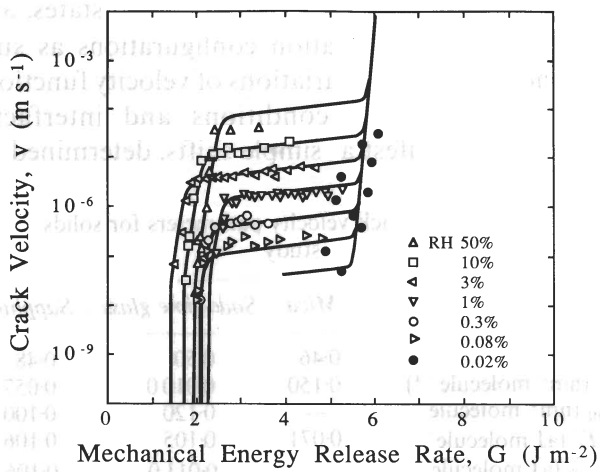

Fig. 6. Crack velocity versus mechanical energy release rate for cracks propagating in sapphire in moist air at specified RH. Constant-load double-cantilever beam data, at room temperature from Ref. 21. Solid curves are theoretical fits.

The curve fits to the data in Figs 2–6 are made by approximating a_0 by a characteristic cleavage-plane bond spacing for each solid[5] and adjusting the following quantities in eqns (2)–(7) (Table 1):

(i) *Threshold.* It is noted that data in the threshold and subthreshold velocity regions are extensively available in the case of mica, less so for glass, and less again for sapphire. For healed cracks in mica in particular (Fig. 2), the zero-velocity energy ${}^{h}W_E$ along the G axis for both matched and misoriented interfaces can be determined with relative accuracy by interpolating between the reversible unloading (negative branch) and reloading (positive branch) curves. Then, using the earlier argument that transitions from virgin to healed interfaces should be manifest as simple curve shifts along the G axis, the corresponding zero-velocity point ${}^{v}W_E$ for the virgin interfaces (Figs 2 and 3) is determined by extrapolation. In the case of glass (Figs 4 and 5), one must resort to extrapolations, for ${}^{v}W_E$, although the water data at different temperatures (Fig. 4) allow these extrapolations to be made with greater confidence. A similar procedure is adopted for sapphire (Fig. 6), but there the sparsity of data at lower velocities means a comparatively high degree of subjectivity in the absolute determinations of ${}^{v}W_E$; justification for extrapolations to zero velocity in this case rests with extraneous evidence for the existence of thresholds in sapphire, e.g. from fatigue limits in strength data using indentation flaws.[19]

In making these interpolations and extrapolations the values of W_E are adjusted independently from each data set at specified water vapour pressure p.

(ii) *Region I.* Parameters α_I and $\Delta F_I^{\cdot}$ are determined from slopes and intercepts of provisional fits to the data in region I in Figs 2–6. In this case single best-fit determinations are made for each solid, i.e. collectively over all water vapour pressures (including liquid water).

(iii) *Region III.* Parameters α_{III} and $\Delta F_{III}^{\cdot}$ are similarly determined for each solid from provisional fits to the data in region III (where available).

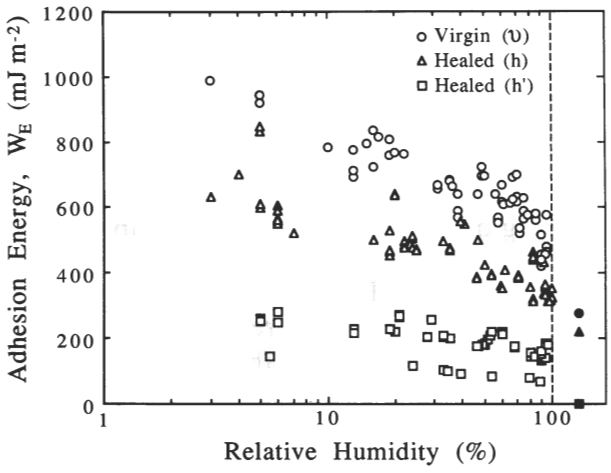

Fig. 7. Adhesion energies W_E for mica from threshold G values, as function of RH (p/p_S, p_S = saturated vapour pressure of water). Data for virgin and healed cracks from Ref. 20. Closed symbols at right of figure are data for water.

(iv) *Region II.* Coefficients λ for each solid are determined from fits to the forward velocity data in the plateau region (where available).

The solid curves in Figs 2–6 are the full v–G functions regenerated from the parameter fits using eqns (6) and (7). It is evident that the analysis describes the transitions between the different regions, and between virgin and healed interfaces.

The adhesion energies W_E from the threshold evaluations are plotted for each of the three solids in Figs 7–9 as a function of relative humidity. Included in the plots for mica are the evaluations for virgin and healed interfaces (matched and misoriented). An analogous data set for healed interfaces in glass from another source[16] are included in Fig. 8.

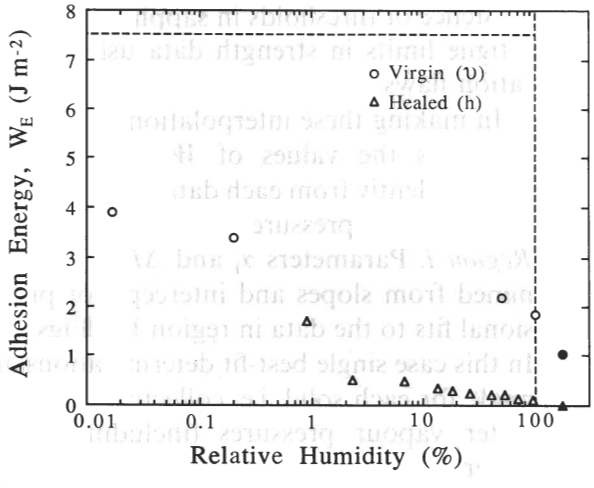

Fig. 8. Adhesion energies W_E for soda-lime glass as function of RH. Data for virgin interfaces from Figs 4 and 5. Data set for healed interfaces from Ref. 16. Closed symbols at right of figure are data for water. Horizontal broken line is adhesion energy for vacuum.

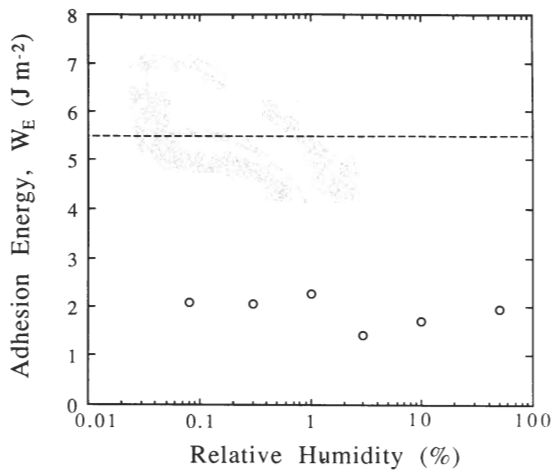

Fig. 9. Adhesion energies W_E for sapphire as function of RH from Fig. 6. Horizontal broken line is adhesion energy for vacuum.

All the other parameters determined from the fitting procedure are listed in Table 1 for each of the three solids.

4 Discussion

The analysis provides a formulation that enables the definition of crack velocity functions for given materials (specifically mica, glass, sapphire) at given water vapour pressures or temperatures. As such, it is appropriate to lifetime predictions in structural design with ceramics. Insofar as the operative mechanisms are not specific (at least in regions I and III), the formulation is *phenomenological*: it is assumed only that the kinetics are determined by atomically localised energy barriers, and that these barriers are stress-enhanced. The analysis nevertheless has a certain generality: it accommodates threshold configurations as equilibrium states, and healing and repropagation configurations as sub-threshold states. The variations of velocity functions with environmental conditions and interfacial history are manifest as simple shifts, determined by

Table 1. Values of crack velocity parameters for solids in this study

Parameter	*Mica*	*Soda-lime glass*	*Sapphire*
a_0 (nm)	0·46	0·50	0·48
α_I (nm^2 molecule^{-1})	0·150	0·0100	0·057
α_{III} (nm^2 molecule^{-1})	—	0·120	0·100
$\Delta F_I^{\ddagger}$ (aJ molecule^{-1})	0·071	0·105	0·106
$\Delta F_{III}^{\ddagger}$ (aJ molecule^{-1})	—	0·0110	0·106
λ (kPa^{-2} s^{-1})	0·30	0·040	0·017

Values of a_0 from Ref. 5. Other parameters from fits to data in Figs 2–6.

appropriate variations in the work of adhesion W_E, along the G axis.

This phenomenological approach has acknowledged limitations. In the absence of *a priori* knowledge of the parameters in the velocity equations empirical 'calibrations' using existing data must be relied upon. Crack velocity results from different laboratories on ostensibly the same materials are notoriously irreproducible, magnified by variations in test geometries and cleavage planes (especially in anisotropic crystals like sapphire[26]), so care needs to be exercised before using calibrations from data at any given set of conditions to predict behaviour at any other condition. Particular caution is needed when making predictions outside the calibration data range.

The authors have chosen to consider somewhat ideal brittle solids without microstructural complications. In many practical ceramics, especially polycrystalline and composite materials, the crack tip may be *shielded* from the external applied loads by microstructural elements which toughen the material as the crack extends[27] (R-curve). The velocity functions determined in the present study remain valid in such cases, but G now identifies explicitly with the energy release rate in the near-field about the crack tip, $G*$. To relate $G*$ to the externally monitored energy release rate, G_A, it is necessary only to evaluate an appropriate shielding term, ΔG ($= G_A - G*$), and thence solve for v–G_A. A description of this kind of shielding has been used elsewhere in an analysis of environmentally induced fatigue properties of alumina ceramics.[28]

It should be evident that there can be little justification in using any such empirically based, phenomenological activation theory in conjunction with macroscopic v–G data to deduce the underlying micromechanics of crack growth. Such unfounded deductions are commonplace, especially in the glass literature. Allusion was made in Section 1 to the traditional attribution of the activation barriers to a chemical reaction at the line of bonds along the crack front;[1,3] but mention was also made there of potentially competitive mechanisms such as interfacial 'lattice' diffusion behind the crack tip[4–6] and 'internal friction' in the near surrounds.[7,8] Independent, definitive identification of such possible mechanisms, and attendant development of more fundamentally based theoretical models of the environmentally modified crack structure within the adhesion zone, are called for. Only then may the prediction of which environments interact with which materials be possible, and thence *a priori* evaluations of crack velocity functions obtained.

The formulation for Region II warrants further consideration. The fitting involved a simple adjustment of λ in eqn (4). Independent estimates of this parameter can be made from eqn (5). Estimates using $l = 0{\cdot}1\ \mu$m for the mean free path of molecule collisions in air at standard atmospheric pressure and temperature, $\eta = 1$ for the site occupancy of adsorbate molecules per surface, $m = 30 \times 10^{-27}$ kg for the mass of a water molecule, and Young's modulus $E = 168$ GPa (mica), 70 GPa (glass) and 400 GPa (sapphire), yield $\lambda = 0{\cdot}057\ \mathrm{kPa^{-2}\,s^{-1}}$ (mica), $0{\cdot}164\ \mathrm{kPa^{-2}\,s^{-1}}$ (glass) and $0{\cdot}026\ \mathrm{kPa^{-2}\,s^{-1}}$ (sapphire). These estimates are within an order of magnitude of the fitted values in Table 1.

Perhaps the most consequential element of this model is the description of velocity thresholds as quiescent states, ultimately determinable in terms of fundamental intersurface forces.[5,6,13] Thus, the $W_E(p)$ plots of Figs 7–9 may be used to determine the concentration dependence of surface and interface energies on interactive species. The specific interpretation of such plots in terms of balanced chemical reaction rates,[1] adsorption isotherms,[8] capillary condensation[20] (including potential effects of dielectric screening[29]), or any other underlying process, remains an issue for analysis elsewhere.

Acknowledgements

This work was funded by the US Office of Naval Research, Ceramics and Metallurgy Program.

References

1. Wiederhorn, S. M., *J. Amer. Ceram. Soc.*, **50** (1967) 407.
2. Lawn, B. R. & Wilshaw, T. R., *Fracture of Brittle Solids*. Cambridge University Press, London, 1975, Chapters 7 and 8.
3. Michalske, T. A., & Freiman, S. W., *Nature*, **295** (1981) 511.
4. Orowan, E., *Nature*, **154** (1944) 341.
5. Lawn, B. R., Roach, D. H. & Thomson, R. M., *J. Mater. Sci.*, **22** (1987) 4036.
6. Lawn, B. R. & Lathabai, S., *Mater. Forum*, **11** (1988) 313.
7. Greenwood, J. A. & Johnson, K. L., *Phil. Mag.*, **A43** (1981) 697.
8. Maugis, D., *J. Mater. Sci.*, **20** (1985) 3041.
9. Lawn, B. R., *Mater. Sci. Eng.*, **13** (1974) 277.
10. Freiman, S. W., *J. Amer. Ceram. Soc.*, **58** (1974) 399.
11. Lawn, B. R., *J. Mater. Sci.*, **10** (1975) 469.
12. Bailey, A. I. & Kay, S. M., *Proc. Roy. Soc., London*, **A301** (1967) 47.
13. Wan, K-T., Aimard, N., Lathabai, S., Horn, R. G. & Lawn, B. R., *J. Mater. Res.*, **5** (1990) 172.
14. Wiederhorn, S. M. & Townsend, P. R., *J. Amer. Ceram. Soc.*, **53** (1970) 486.
15. Stavrinidis, B. & Holloway, D. G., *Phys. Chem. Glasses*, **24** (1983) 19.

16. Michalske, T. A. & Fuller, E. R., *J. Amer. Ceram. Soc.*, **68** (1985) 586.
17. Hockey, B. J. & Lawn, B. R., *J. Mater. Sci.*, **10** (1975) 1275.
18. Rice, J. R., *J. Mech. Phys. Solids*, **26** (1978) 61.
19. Cook, R. F., *J. Mater. Res.*, **1** (1986) 852.
20. Wan, K.-T. & Lawn, B. R., *Acta Metall.*, (in press).
21. Wiederhorn, S. M., In *Mechanical and Thermal Properties of Ceramics*, ed. J. B. Wachtman. National Bureau of Standards, Special Technical Publication 303 NBS, Gaithersburg, MD., 1969, p. 217.
22. Glasstone, S., Laidler, K. J. & Eyring, H., *The Theory of Rate Processes*. McGraw-Hill, New York, 1941.
23. Fuller, E. R., Lawn, B. R. & Thomson, R. M., *Acta Metall.*, **28** (1980) 1407.
24. Wiederhorn, S. M. & Bolz, L. H., *J. Amer. Ceram. Soc.*, **53** (1970) 543.
25. Freiman, S. W., White, G. S. & Fuller, E. R., *J. Amer. Ceram. Soc.*, **68** (1985) 108.
26. Cannon, R. M., In *Advances in Ceramics*, Vol. 10, ed. W. D. Kingery. American Ceramic Society, Columbus, 1984, p. 818.
27. Lawn, B. R., *J. Amer. Ceram. Soc.*, **66** (1983) 83.
28. Lathabai, S. & Lawn, B. R., *J. Mater. Sci.*, **24** (1989) 4298.
29. Gaines, G. L. & Tabor, D., *Nature*, **178** (1956) 1304.
30. Marshall, D. B. & Lawn, B. R., *J. Amer. Ceram. Soc.*, **63** (1980) 532.
31. Gupta, P. K., & Jubb, N. J., *J. Amer. Ceram. Soc.*, **64** (1981) C-112.
32. Marshall, D. B. & Lawn, B. R., *J. Mater. Sci.*, **14** (1979) 2001.
33. Lawn, B. R., Evans, A. G. & Marshall, D. B., *J. Amer. Ceram. Soc.*, **63** (1980) 574.

Appendix

Results of crack velocity measurements using Vickers indentation flaws are used to supplement the existing literature data for soda-lime glass in Figs 4 and 5. The procedure is to observe post-indentation virgin crack growth under the exclusive action of the residual contact stress field.[30,31] Because the residual-field system is essentially stable[32] the crack driving force falls off with crack extension, so the system progresses naturally down the v–G curve. As such, the configuration is especially suited to extending the database into the threshold region.

Experiments were run as follows. Vickers indentations at specified load P were placed in polished, annealed soda-lime glass surfaces, in a specified environment and at a specified temperature. Several indentations could be made on a given test surface. The post-contact crack evolution $c(t)$ was followed in an optical microscope, over a time interval ≈ 10 s to ≈ 1 year. The estimated relative accuracy in measuring the position of the crack tip was $\approx 2\,\mu$m.

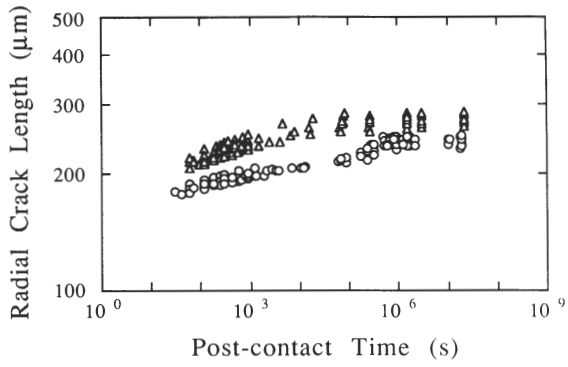

Fig. A1. Radial crack length versus post-contact time for Vickers indentations at load $P = 29{\cdot}4$ N in soda-lime glass in water (△) and air (○) at RH 50–60%, at room temperature. Data from several indentation cracks. (Velocities measured from increments in crack size in individual runs, to eliminate the considerable crack-to-crack variation evident in these plots.)

Representative crack length versus post-indentation time plots are shown in Fig. A1, for runs in water and air at room temperature. The plateau at long times is indicative of threshold behaviour.

The v–G data were extracted from such data sets as follows:

(i) Velocities were determined from measurements of radial crack growth increments over successive time intervals for each indentation crack. (At lower velocities it was necessary to increase these time intervals, in order that the crack increments exceed the resolution limit.)

(ii) Mechanical energy release rates were determined from the standard stress-intensity factor solution for well-developed indentation cracks

$$K = \chi P/c^{3/2} \tag{A1}$$

in conjunction with the connecting plane-strain relation

$$G = K^2(1 - \nu^2)/E \tag{A2}$$

with χ an indentation coefficient, E Young's modulus and ν Poisson's ratio.[32,33] The indentation coefficient for soda-lime glass is here expediently adjusted to the value $\chi = 0{\cdot}040$ to match Wiederhorn's v–K baseline results for glass in water so as to ensure self-consistency in the data sets in Figs 4 and 5.